Filomat 31:8 (2017), 2231–2241
DOI 10.2298/FIL1708231Q

Published by Faculty of Sciences and Mathematics,
University of Niš, Serbia
Available at: http://www.pmf.ni.ac.rs/filomat

Harmonic Shears and Numerical Conformal Mappings

Tri Quach[a]

[a] *Aalto University, Department of Mathematics and Systems Analysis, P.O. Box 11100, FI-00076 Aalto, Finland.*

Abstract. In this article we introduce a numerical algorithm for finding harmonic mappings by using the *shear construction* introduced by Clunie and Sheil-Small in 1984. The MATLAB implementation of the algorithm is based on the numerical conformal mapping package, the Schwarz-Christoffel toolbox, by T. Driscoll. Several numerical examples are given. In addition, we discuss briefly the minimal surfaces associated with harmonic mappings and give a numerical example of minimal surfaces.

1. Introduction

A complex-valued harmonic function $f = u + iv$, defined on the unit disk $\mathbb{D}$, is called a *harmonic mapping* if the coordinate function u and v are real harmonic, and it maps $\mathbb{D}$ univalently onto a domain $\Omega \subset \mathbb{C}$. Note that it is not required that the real part and the imaginary part of f are harmonic conjugate functions, i.e., satisfy the Cauchy-Riemann equations. In 1984, Clunie and Sheil-Small [5] showed that many classical results for conformal mappings have natural analogues for harmonic mappings, and hence they can be regarded as a natural generalization of conformal mappings. Since then, this class of mappings has attracted considerable interest in complex analysis, see e.g. [10].

An important method for studying geometric properties of harmonic mappings is called harmonic shearing. Since its introduction in [5], it has been researched by many authors. For example, Greiner [13] studied harmonic shears of conformal mappings from the unit disk onto infinite strips and other domains. Shearing of conformal mappings from the unit disk onto regular polygonal domains have been studied in the paper by Driver and Duren [9], and by the author with Ponnusamy and Rasila [27].

The shear construction makes use of a conformal mapping φ and an analytic dilatation ω. For required assumptions for the dilatation ω, see Section 2.

An applet [28] for exploring harmonic shears with user defined conformal mappings is written by Rolf and examples are given in [6]. However, no accuracy tests against analytic form have been given in [6]. Note that, the applet requires an analytic expression for the conformal mapping.

In this paper, the Schwarz-Christoffel toolbox by Driscoll [7] is used to provide a conformal mapping for the presented numerical method for harmonic shear. The toolbox computes a conformal mapping from the unit disk $\mathbb{D}$ onto a polygonal domain. See [8, 29] for details for the construction of a conformal mapping.

2010 *Mathematics Subject Classification*. Primary 30C99; Secondary 30C30, 31A05, 65E05
Keywords. Harmonic univalent mappings, convex along horizontal directions, harmonic shear, numerical method, conformal mappings, minimal surfaces.
Received: 29 January 2015; Accepted: 15 July 2015
Communicated by Miodrag Mateljevic
The author was supported by a grant (ma2011n25) from the Magnus Ehrnrooth Foundation.
Email address: tri.quach@aalto.fi (Tri Quach)

In principle, other methods can be used to obtain conformal mappings as well. An example of a numerical method, that does not involve the Schwarz-Christoffel formula, is the Zipper algorithm of Marshall [20, 21]. A method involving the harmonic conjugate function is presented in [16, pp. 371-374].

An algorithm using the harmonic conjugate function and properties of quadrilateral is given by the author in a joint work with Hakula and Rasila [14]. The algorithm is based on properties of the conformal modulus originating on the theory of quasiconformal mappings [1, 18, 25]. The method is suitable for simply and doubly connected domains, which may have curved boundaries and even cusps. The implementation of the algorithm is based on the *hp*-FEM from [15].

An important application of harmonic mappings is related to minimal surfaces. A harmonic function $f = h + \overline{g}$ can be lifted to a minimal surface if and only if the dilatation ω is the square of an analytic function. Suppose that $\omega = q^2$ for some analytic function q in the unit disk $\mathbb{D}$. Then the corresponding minimal surface has the form

$$\{u, v, w\} = \{\operatorname{Re} f, \operatorname{Im} f, 2 \operatorname{Im} \psi\},$$

where

$$\psi(z) = \int_0^z q(\zeta) \frac{\varphi(\zeta)}{1 - \omega(\zeta)}\, d\zeta.$$

The approach taken in this paper is based on the Weierstrass-Enneper representation. For further information about the relation between harmonic mappings and minimal surfaces can be found from [10]. Minimal surfaces are closely related to many interesting phenomena in natural science and engineering, from mathematical models of soap bubble surfaces [17], to topics in molecular engineering [3], and tensile structures [4]. For a further reading on minimal surfaces and their applications see, e.g., [23, 24].

In this paper, the MATLAB visualisations of harmonic mappings are kept as close to the original images (cf. [9, 27]) as possible for easier comparison. Besides given illustrations, one can enhance the visualisations, e.g., by using phase portrait method [30, 31] or by using domain coloring method [19, 26].

2. Harmonic Mappings

A harmonic mapping in $\mathbb{D}$ has a canonical presentation $f = h + \overline{g}$, where h and g are analytic in $\mathbb{D}$ and $g(0) = 0$. A harmonic mapping $f = h + \overline{g}$ is called *sense-preserving* if the Jacobian $J_f = |h'|^2 - |g'|^2$ is positive in $\mathbb{D}$. Then f has an *analytic dilatation* $\omega = g'/h'$ such that $|\omega(z)| < 1$ for $z \in \mathbb{D}$. For basic properties of harmonic mappings, see [10].

A domain $\Omega \subset \mathbb{C}$ is said to be *convex in the horizontal direction* (CHD) if its intersection with each horizontal line is connected (or empty). A univalent harmonic mapping is called a CHD mapping if its range is a CHD domain. Construction of a harmonic mapping f with prescribed dilatation ω can be done by the *shear construction* devised by Clunie and Sheil-Small [5]. For reader's convenience, we recall the construction along with its basic properties.

Theorem 2.1. *Let $f = h + \overline{g}$ be a harmonic and locally univalent in the unit disk $\mathbb{D}$. Then f is univalent in $\mathbb{D}$ and its range is a* CHD *domain if and only if $h - g$ is a conformal mapping of $\mathbb{D}$ onto a* CHD *domain.*

Proof. See, e.g., [10, p. 37]. □

Suppose that φ is a CHD conformal mapping. For a given dilatation ω, the harmonic shear $f = h + \overline{g}$ of φ is obtained by solving the differential equations

$$\begin{cases} h' - g' = \varphi', \\ \omega h' - g' = 0. \end{cases}$$

From the above equations, we obtain

$$h(z) = \int_0^z \frac{\varphi'(\zeta)}{1 - \omega(\zeta)}\, d\zeta. \tag{1}$$

For the anti-analytic part g, we have

$$g(z) = \int_0^z \omega(\zeta)\frac{\varphi'(\zeta)}{1-\omega(\zeta)}\,d\zeta. \tag{2}$$

Observe that f can also be written as

$$f(z) = 2\,\mathrm{Re}\left[\int_0^z \frac{\varphi'(\zeta)}{1-\omega(\zeta)}\,d\zeta\right] - \overline{\varphi(z)}. \tag{3}$$

The last equation is useful if the conformal mapping φ is known.

3. Numerical Aspects

Solving (3) numerically, we shall use the change of variable $\zeta = zt$. Thus the analytic part of f takes the following form

$$h(z) = \int_0^1 \frac{\varphi'(zt)}{1-\omega(zt)} z\,dt. \tag{4}$$

Then for the harmonic shear f, we have

$$f(z) = 2\,\mathrm{Re}\left[\int_0^1 \frac{\varphi'(zt)}{1-\omega(zt)} z\,dt\right] - \overline{\varphi(z)}. \tag{5}$$

Above integrals can be computed numerically, for example, by using the Gauss quadrature.

3.1. Gauss Quadrature

The key idea behind the Gauss quadrature is to choose the interpolation nodes in order to maximize the degree of exactness of the quadrature rule. In the Gauss quadrature one will consider integrals of the form

$$I(g) = \int_a^b g(x)\,dx = \int_a^b f(x)\eta(x)\,dx = \sum_{j=1}^{N} w_j f(x_j), \tag{6}$$

where $\{w_j, x_j\}_{j=1}^N$ is a quadrature rule corresponding to the weight function η. In [12], Golub and Welsch gave algorithms to the Gauss quadrature for different weight functions. More in-depth discussion of the Gauss quadrature can be found, e.g., in [11, Section 5.3].

In our case, we have a singularity of the form $1/(1-\omega(z))$ caused by the dilatation. For some choices of dilatation, we can use the appropriate Gauss quadrature to deal with the singularity. However, in this article, we shall use the Gauss-Kronrod quadrature, which is also build in MATLAB. The Gauss-Kronrod quadrature is a generalization of a pure Gaussian quadrature and the method adds additional nodes to the Gauss rule with a way to control the error. It should also be noted that, the Gauss-Kronrod quadrature does not take possible singularities into account. For futher discussion of the Gauss-Kronrod quadrature, see [11, pp. 299–300].

3.2. Setup of the Validation Test

Numerical experiments are divided into two meshing of the unit disk. For the first part, the following mesh of the form $re^{i\theta}$, where $r = \{k/20 : k = 0, 1, 2, \ldots, 20\}$ and $\theta = \{2\pi k/40 : k = 0, 1, 2, \ldots, 40\}$, is used. The second mesh is refined near the boundary of the unit disk, where $r = \{(990+k)/1000 : k = 0, 1, 2, \ldots, 10\}$ and meshing for the angle is the same as in the first mesh.

Validation of the numerical scheme is run against the analytic representation of the harmonic mappings. All conformal mappings obtained by the SC toolbox are computed with the precision setting: `precision = 1e-14`.

Note that, by using (3), one have two sources of errors. The first one comes from the integral presentation of h and the second source of error comes from the conformal mapping φ itself.

In the unit disk, the comparison of the harmonic mapping is done by using the following test function

$$\text{test} = |f - Q(f)|, \tag{7}$$

where f is the analytic expression of the harmonic mapping and $Q(f)$ is given by the quadrature. Note that, by (5), we may write the test function as follows

$$\text{test} = |f - Q(f)| \leq 2\,|\text{Re}(h - Q(h))| + |\varphi - Q(\varphi)|, \tag{8}$$

where $Q(h)$ and $Q(\varphi)$ are obtained by the Gauss-Kronrod quadrature and the SC toolbox, respectively.

4. Examples of Polygonal Mappings

In this section, we consider polygonal examples. Let the conformal mapping be (see [22, p. 196])

$$\varphi(z) = \int_0^z (1 - \zeta^n)^{-2/n}\, d\zeta,$$

which maps the unit disk $\mathbb{D}$ onto a regular n-gon. In [9], Driver and Duren discussed the harmonic shear of φ with the dilatation $\omega(z) = z^n$. They studied other dilatation choices as well. The author considered the dilatation $\omega(z) = z^{2n}$ in a joint work with Ponnusamy and Rasila [27].

4.1. Analytic Form

In [9], it was shown that for the dilatation $\omega(z) = z^n$, the harmonic shear of φ is given by

$$\begin{cases} h(z) = zF\left(1 + \dfrac{2}{n}, \dfrac{1}{n}; 1 + \dfrac{1}{n}; z^n\right), \\ g(z) = \dfrac{z^{n+1}}{n+1} F\left(1 + \dfrac{2}{n}, 1 + \dfrac{1}{n}; 2 + \dfrac{1}{n}; z^n\right), \end{cases}$$

where $F(a, b; c; z)$ if the Gaussian hypergeometric function. The function is defined as follows

$$F(a, b; c; z) = 1 + \sum_{n=1}^{\infty} \frac{(a)_n (b)_n}{n!(c)_n} z^n, \quad |z| < 1,$$

where

$$(\alpha)_n = \alpha(\alpha + 1) \cdots (\alpha + n - 1) = \frac{\Gamma(\alpha + n)}{\Gamma(\alpha)}, \quad \alpha \in \mathbb{C},$$

is the Pochhammer symbol. For $\text{Re}\, c > \text{Re}\, b > 0$, this can also be written as the Euler integral

$$F(a, b, c; z) = \frac{\Gamma(c)}{\Gamma(b)\Gamma(c - b)} \int_0^1 t^{b-1}(1 - t)^{c-b-1}(1 - zt)^{-a}\, dt.$$

In case of $\omega(z) = z^{2n}$, the harmonic shear is shown, in [27], to be

$$\begin{cases} h(z) = zF_1\left(\dfrac{1}{n}, 1 + \dfrac{2}{n}, 1; 1 + \dfrac{1}{n}; z^n, -z^n\right), \\ g(z) = \dfrac{z^{2n+1}}{2n+1} F_1\left(2 + \dfrac{1}{n}, 1 + \dfrac{2}{n}, 1; 3 + \dfrac{1}{n}; z^n, -z^n\right), \end{cases}$$

where $F_1(a, b_1, b_2; c; x, y)$ is the first Appell hypergeometric function [2, p. 73], which is defined by

$$F_1(a, b_1, b_2; c; x, y) = \sum_{k=0}^{\infty} \sum_{l=0}^{\infty} \frac{(a)_{k+l}(b_1)_k(b_2)_l}{(c)_{k+l}\, k!\, l!} x^k y^l,$$

Appell hypergeometric functions can be given by Euler's integral as follows [2, p. 77]:

$$F_1(a, b_1, b_2; c; x, y) = \frac{\Gamma(c)}{\Gamma(a)\Gamma(c-a)} \int_0^1 t^{a-1}(1-t)^{c-a-1}(1-xt)^{-b_1}(1-yt)^{-b_2}\, dt,$$

where $\operatorname{Re} c > \operatorname{Re} a > 0$.

4.2. Example

Let $\omega(z) = z^{2n}$, $n = 4$. The reason we chose this dilatation is that, in (1) we have eight singularities and it reveals the accuracy of our algorithm and as well as the accuracy of the SC toolbox. In Figure 1, we have reproduced the figures from [27] and numerically computed images using the presented algorithm.

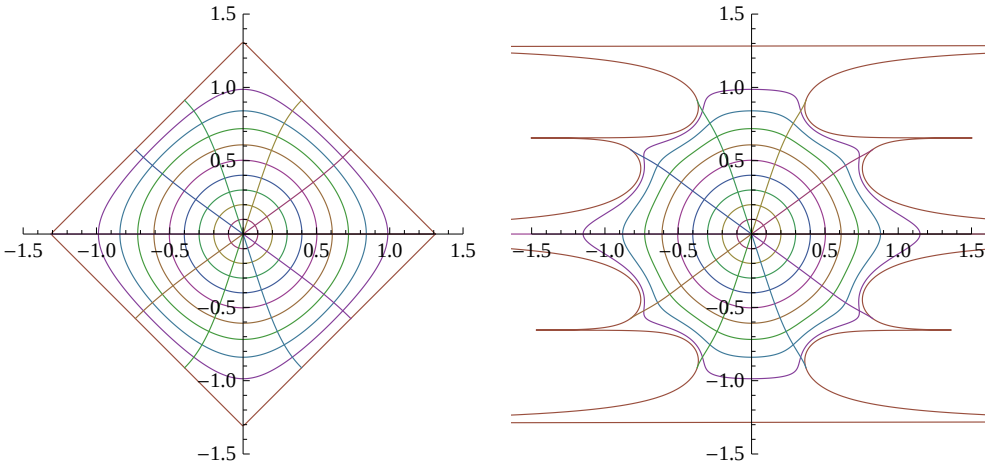

(a) Visualisation of an analytic form given by Mathematica.

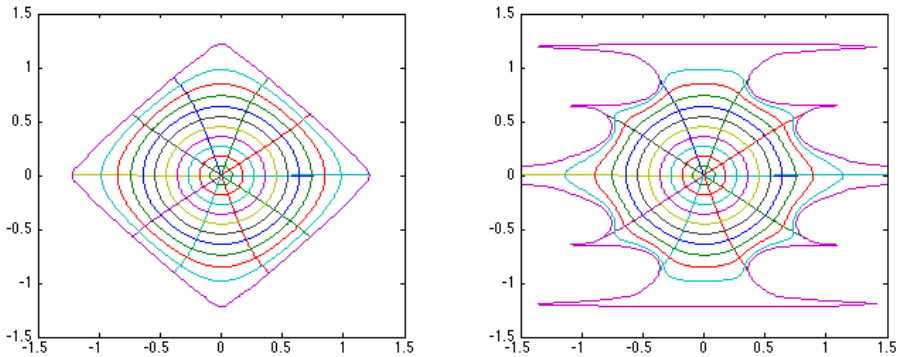

(b) A numerical version computed by MATLAB. Note that, the radius of the outermost circle is chosen to be 0.99, to avoid extensive amount of visual artefacts.

Figure 1: Conformal mapping φ of the unit disk $\mathbb{D}$ onto a square and its harmonic shears with the dilatation $\omega(z) = z^8$.

In Figure 2, we have the error of the test function (7) of the harmonic shear f given in the logarithmic scale (with base 10). Note that, the error is given in the pre-image form, so that the figure can be shown in a more compact manner. Also the error corresponding to the second mesh can be stretch as the boundary the unit disk. In this process, the readability of the picture would be lost due to the poor resolution, and thus, the error is given in the form of a rectangle.

White areas in illustrations correspond to the loss of accuracy at singularities due to roots of the $1 - z^8$. In the second mesh, near the boundary, we see that the rapid loss of accuracy occurs at the neighbourhood of the singularities.

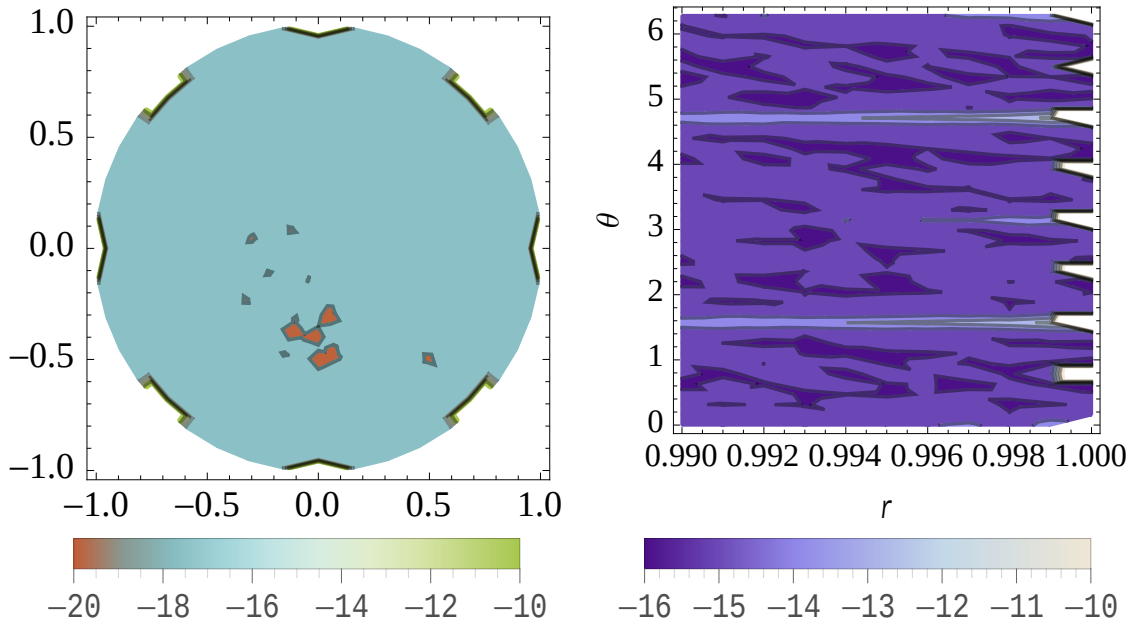

Figure 2: Error analysis of the harmonic shear of conformal mapping φ of the unit disk $\mathbb{D}$ onto a square with the dilatation $\omega(z) = z^8$. On the left hand side, we have the error of the first mesh, and on the right hand side, we the corresponding error near the boundary of the unit disk. Results are obtained by taking the logarithm (with base 10) of the test function (7).

In Figure 3, we have errors corresponding to right hand side of the (8). The conformal mapping itself has 4 singularities arising from the roots of $1 - \zeta^4$. The loss of accuracy is around 4 digits in this particular example, which is nuisance but a not severe obstacle. Unfortunately, for the analytic part h of f, even the leading digit is wrong at singularities most of the time. This can be improve if the type of singularities are known and the quadrature is adapted to take this information into account. Elsewhere the performance shows no significant shortcomings.

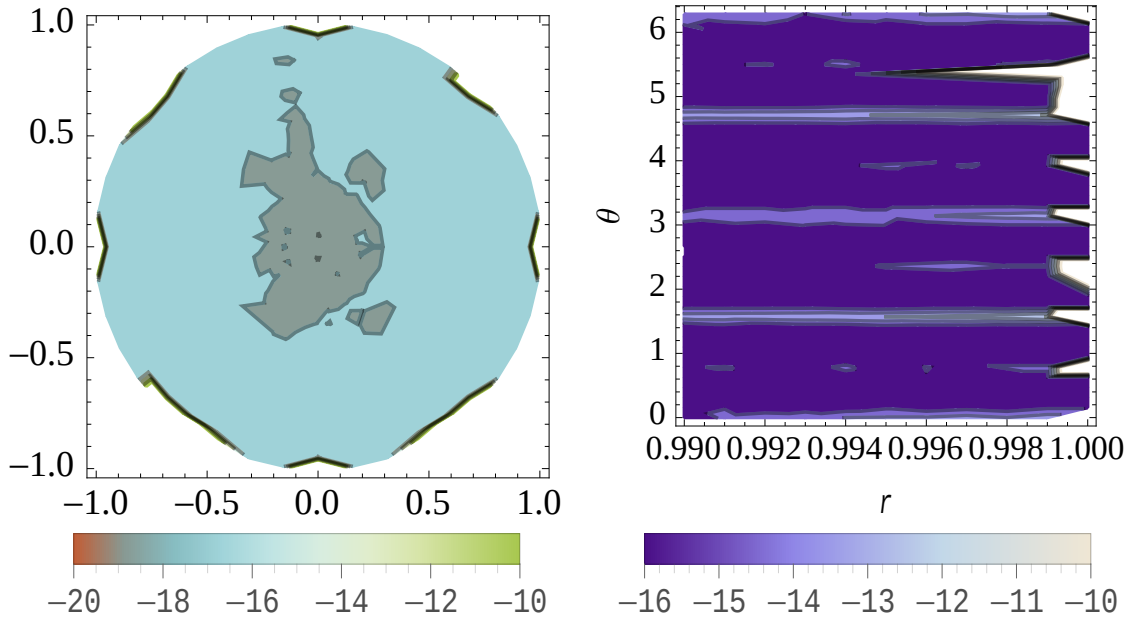

(a) Error of the analytic part h of f in form of $2\,|\mathrm{Re}(h - Q(h))|$.

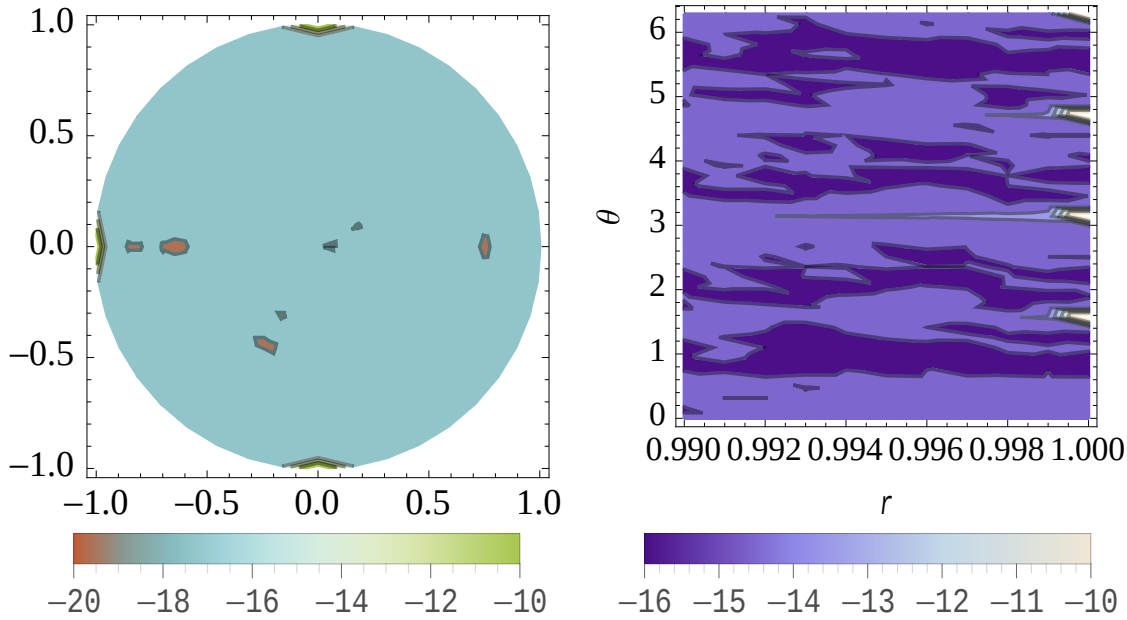

(b) Error analysis of the conformal mapping φ from the unit disk onto a square.

Figure 3: Error analysis of the analytic part h of f and the conformal mapping φ in the case of the harmonic shear of conformal mapping φ of the unit disk $\mathbb{D}$ onto a square with the dilatation $\omega(z) = z^8$. Results are obtained by taking the logarithm (with base 10) of the corresponding part of the test function (8).

4.3. *Polygonal Shears with Other Dilatations*

We shall reproduce the images from [9] for the dilation $\omega(z) = z^n$ and from [27] using dilatition $\omega(z) = z^{2n}$ with our numerical algorithm along with the error analysis. In Figure 4, we have $n = 3$. For illustrastions

for $n = 5$, see Figure 5.

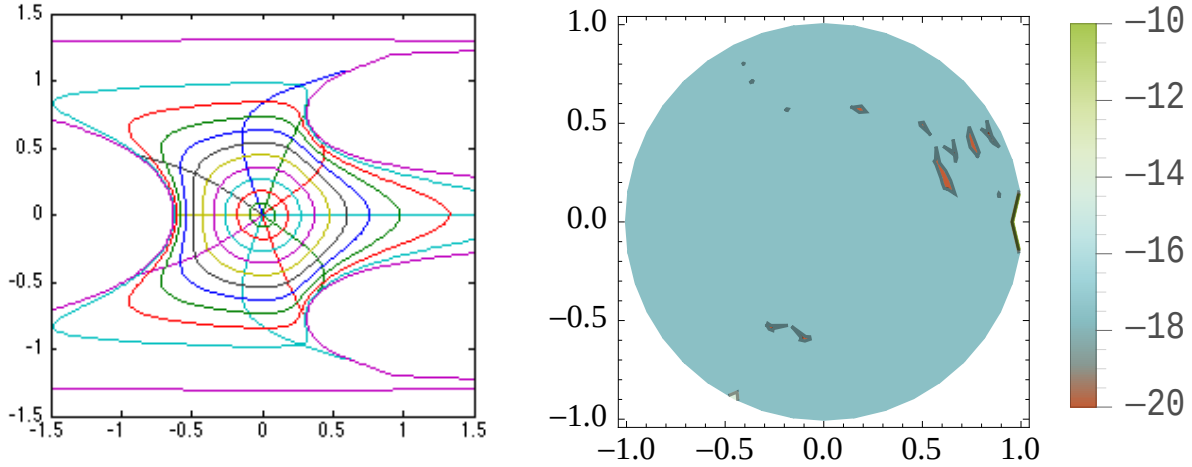

(a) Dilatation $\omega(z) = z^3$.

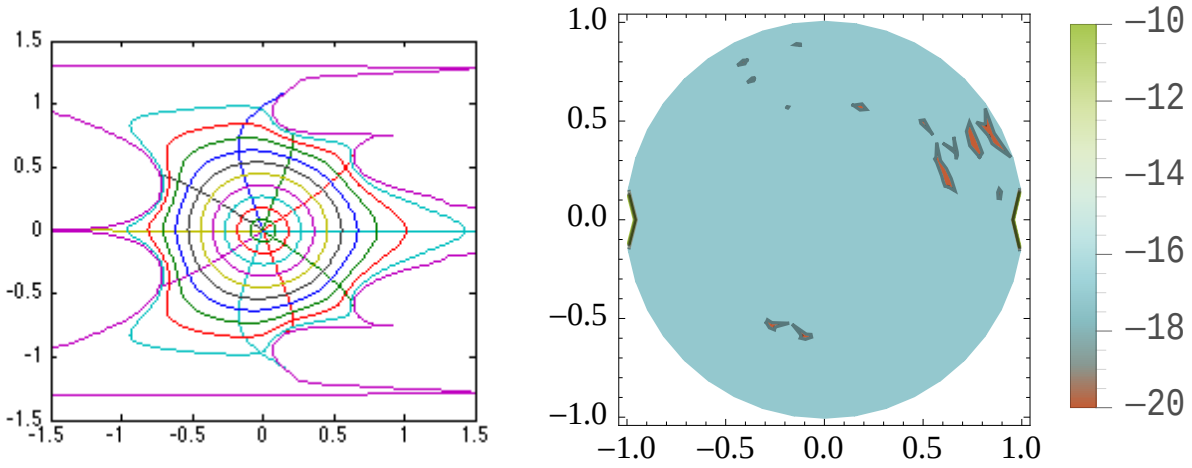

(b) Dilatation $\omega(z) = z^6$.

Figure 4: Reproduction from [9] and [27] of the conformal mapping φ of the unit disk $\mathbb{D}$ onto a triangle and its harmonic shears with dilatation $\omega(z) = z^3, z^6$, respectively. The error is given in the logarithmic (base 10) scale. Note that, the radius of the outermost circle is chosen to be 0.99, to avoid extensive amount of visual artefacts.

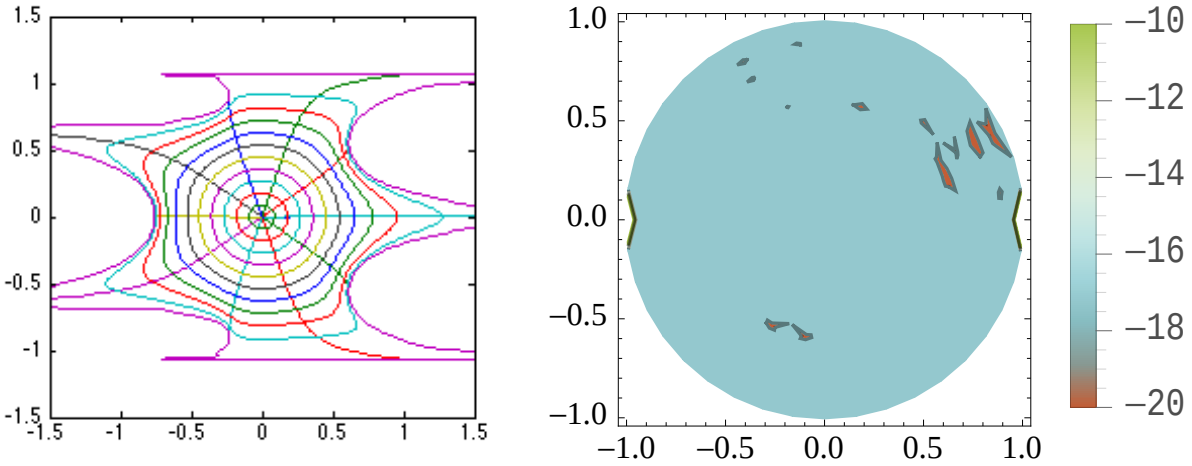

(a) Dilatation $\omega(z) = z^5$.

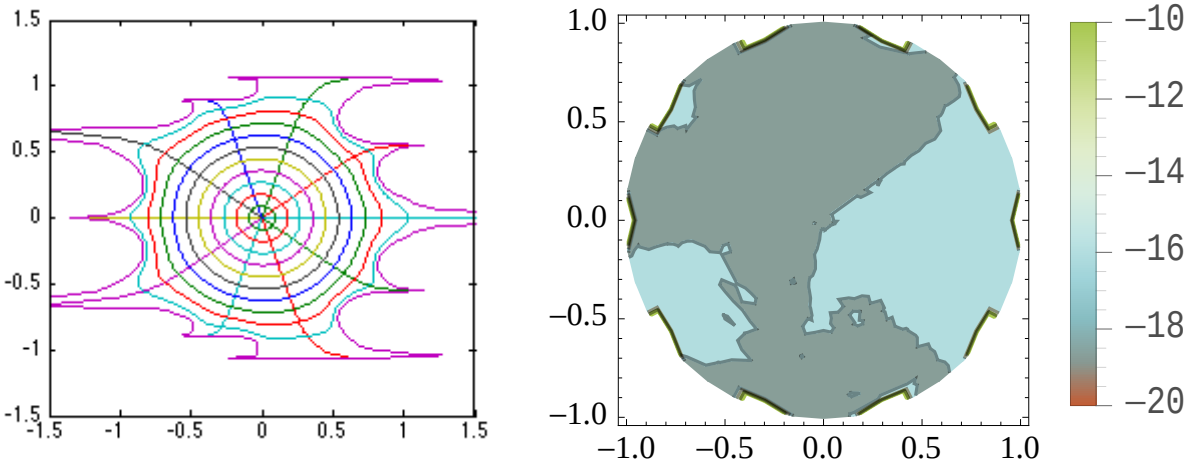

(b) Dilatation $\omega(z) = z^{10}$.

Figure 5: Reproduction from [9] and [27] of the conformal mapping φ of the unit disk $\mathbb{D}$ onto a pentagon and its harmonic shears with dilatation $\omega(z) = z^5, z^{10}$, respectively. The error is given in the logarithmic (base 10) scale. Note that, the radius of the outermost circle is chosen to be 0.99, to avoid extensive amount of visual artefacts.

5. Minimal Surfaces

It is known that a harmonic function $f = h + \overline{g}$ can be lifted to a minimal surface if and only if the dilatation ω is the square of an analytic function. Suppose that $\omega = q^2$ for some analytic function q in the unit disk $\mathbb{D}$. Then the corresponding minimal surface has the form

$$\{u, v, w\} = \{\mathrm{Re}\, f, \mathrm{Im}\, f, 2\,\mathrm{Im}\, \psi\},$$

where

$$\psi(z) = \int_0^z q(\zeta)\frac{\varphi(\zeta)}{1-\omega(\zeta)}\, d\zeta.$$

In [9], Driver and Duren computed ψ for a conformal mapping φ from unit disk onto a n-gon with dilatation $\omega(z) = z^n$. Computation is done with assumption that n is even. In this case the minimal surface lifting is given by

$$\psi(z) = \frac{2z^{1+1/n}}{n+2} F\left(1 + \frac{2}{n}, \frac{1}{2} + \frac{1}{n}; \frac{3}{2} + \frac{1}{n}; z^n\right).$$

In Figure 6, we have a illustration for $n = 4$ given by the exact solution and the numerical scheme.

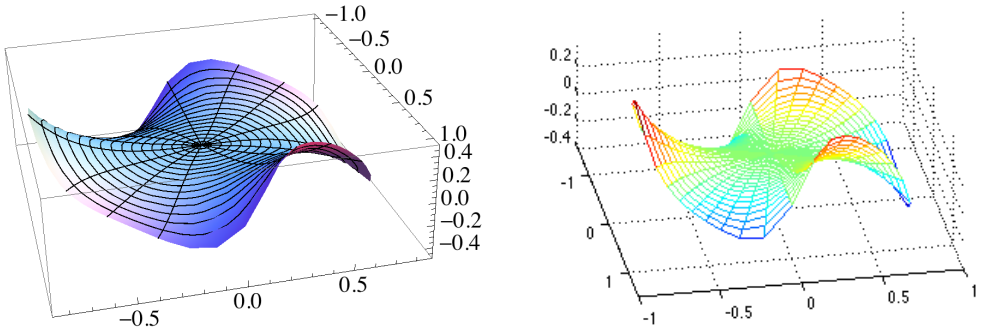

Figure 6: Minimal surface of the conformal mapping φ of unit disk onto n-gon with a dilatation $\omega(z) = z^n$, $n = 4$. On the left hand side, we have a illustration given by exact solution. In comparison, on the right hand side, we have a numerically computed version of the minimal surface. To give a sensible illustration, we have chosen the outermost circle's radius to be 0.8. This example is a reproduction from [9].

6. Conclusions

In this article, we have given an algorithm to numerically shear CHD conformal mappings. Required integrations are done using a standard Gauss-Kronrod quadrature. From given examples against analytic expression, we found that our numerical method's performance is satisfactory on all mesh points we have considered except singularities. The accuracy can be improved if the type of the singularity is known and the algorithm is tweaked to work around it.

References

[1] L.V. Ahlfors, Conformal invariants: topics in geometric function theory, McGraw-Hill Book Co., 1973.
[2] W.N. Bailey, Generalized hypergeometric series, Cambridge Tracts in Mathematics and Mathematical Physics, No. 32 Stechert-Hafner, Inc., New York, 1964.
[3] J.V. Barth, G. Constantini, K. Kern, Engineering atomic and molecular nanostructures at surfaces, Nature 437 (2005) 671–679.
[4] H. Berger, Light structures, structures of light: The art and engineering of tensile architecture, (2nd edition), AuthorHouse, 2005.
[5] J. Clunie, T. Sheil-Small, Harmonic univalent functions, Ann. Acad. Sci. Fenn. Ser. A I Math. 9 (1984) 3–25.
[6] M. Dorff, Anamorphosis, mapping problems, and harmonic univalent functions, Explorations in Complex Analysis, 197–269, Math. Assoc. of America, Inc., Washington, DC, 2012.
[7] T.A. Driscoll, Schwarz-Christoffel toolbox for MATLAB, `http://www.math.udel.edu/~driscoll/software/SC/`.
[8] T.A. Driscoll, L.N. Trefethen, Schwarz-Christoffel Mapping, Cambridge Monographs on Applied and Computational Mathematics, 8. Cambridge University Press, 2002.
[9] K. Driver, P. Duren, Harmonic shears of regular polygons by hypergeometric functions, J. Math. Anal. Appl. 239(1) (1999) 72–84.
[10] P. Duren, Harmonic Mappings in the Plane, Cambridge Tracts in Mathematics, 156. Cambridge University Press, 2004.
[11] A. Gil, J. Segura, N.M. Temme, Numerical methods for special functions, SIAM, Philadelphia, PA, 2007.
[12] G.H. Golub, J.H. Welsch, Calculation of Gauss Quadrature Rules, Math. Comp. 23(106) (1969) 221–230.
[13] P. Greiner, Geometric properties of harmonic shears, Comput. Methods Funct. Theory 4(1) (2004) 77–96.
[14] H. Hakula, T. Quach, A. Rasila, Conjugate Function Method for Numerical Conformal Mappings, J. Comput. Appl. Math. 237(1) (2013) 340–353.

[15] H. Hakula, A. Rasila, M. Vuorinen, On moduli of rings and quadrilaterals: algorithms and experiments, SIAM J. Sci. Comput. 33(1) (2011) 279–302.
[16] P. Henrici, Applied and computational complex analysis. Vol. 3, Discrete Fourier analysis—Cauchy integrals—construction of conformal maps—univalent functions. Pure and Applied Mathematics (New York). A Wiley-Interscience Publication. John Wiley & Sons, Inc., New York, 1986.
[17] C. Isenberg, The Science of Soap Films and Soap Bubbles, republication of the 1978 edition, Dover Publications, Mineola, New York, 1992.
[18] O. Lehto, K.I. Virtanen, Quasiconformal mappings in the plane, Springer, Berlin, 1973.
[19] H. Lundmark, Visualizing complex analytic functions using domain coloring, accessed 25 March 2015, http://www.mai.liu.se/~hanlu09/complex/domain_coloring-unicode.html.
[20] D.E. Marshall, Zipper, Fortran Programs for Numerical Computation of Conformal Maps, and C Programs for X-11 Graphics Display of the Maps. Sample pictures, Fortran, and C code available online at http://www.math.washington.edu/~marshall/personal.html.
[21] D.E. Marshall, S. Rohde, Convergence of a variant of the zipper algorithm for conformal mapping, SIAM J. Numer. Anal. 45(6) (2007) 2577–2609 (electronic).
[22] Z. Nehari, Conformal mapping, republication of the 1952 edition, Dover Publications, Inc., New York, 1975.
[23] J.C.C. Nitsche, ectures on Minimal Surfaces, Vol. I, Cambridge University Press, Cambridge, 1989.
[24] R. Osserman, A Survey of Minimal Surfaces, (2nd edition), Dover Publications, Mineola, New York, 1986.
[25] N. Papamichael, N.S. Stylianopoulos, Numerical Conformal Mapping: Domain Decomposition and the Mapping of Quadrilaterals, World Scientific Publishing Company, 2010.
[26] K. Poelke, K. Poltier, Lifted Domain Coloring, Computer Graphics Forum 28(3) (2009) 735–742.
[27] S. Ponnusamy, T. Quach, A. Rasila, Harmonic Shears of Slit and Polygonal Mappings, Applied Mathematics and Computation 233 (2014) 588–598.
[28] J. Rolf, ShearTool applet, http://www.jimrolf.com/explorationsInComplexVariables/chapter4.html.
[29] L.N. Trefethen, Numerical computation of the Schwarz-Christoffel transformation, SIAM J. Sci. Statist. Comput. 1(1) (1980) 82–102.
[30] E. Wegert, Visual complex functions: An introduction with phase portraits, Springer, Basel, 2012.
[31] E. Wegert, Complex functions and images, Comput. Methods Funct. Theory 13(1) (2013) 3–10.